European Journal of Mechanical Engineering Research, 10(2),32-45, 2023

Print ISSN: 2055-6551(Print)

Online ISSN: 2055-656X(Online)

Website: https://www.eajournals.org/

Publication of the European Centre for Research Training and Development -UK

Analytical Comparison of Top and Bottom Jet Impingement Controlled Cooling Configuration Using CFD

[1]Thomas O. Onah, [2]Azubuike M. Nwankwo, [3]Christian C. Aka

[1,3]Department of Mechanical and Production Engineering, Enugu State University of Science and Technology, Enugu

[2]Department of Works and Engineering Services, Federal Polytechnic, Oko, Anambra

doi: https://doi.org/10.37745/ejmer.2014/vol10n23245 Published December 26, 2023

Citation: Onah T.O., Nwankwo A.M., Aka C.C. (2023) Analytical Comparison of Top and Bottom Jet Impingement Controlled Cooling Configuration Using CFD, *European Journal of Mechanical Engineering Research*, 10 (2),32-45

ABSTRACT: *Jet impingement heat transfer was studied using top and bottom surface stationary cooling configuration. Using rectangular steel plates of 230mm by 120mm by 12mm, and single jet diameters of 10mm and 40mm with impingement gaps of 115mm and 155mm. Experimental data were reduced by lumped thermal mass analysis model for calculating convective heat transfer coefficient and ANSYS CFD software was used to validate experimental results. The results analyzed by lumped thermal mass analytical showed that, for a diameter 10mm and impingement gap of 115mm, the Top surface showed better-controlled cooling with a 63% difference, and at impingement gap, 155mm top surface maintained better cooling with a 66% difference for a diameter 40mm. The calculated convective heat transfer coefficient increases with an increase in pipe diameter and a corresponding increase in impingement gaps in both cooling processes. The CFD results revealed maximum heat fluxes of 22518W/m^2 and 6742.8w/m^2 for the top at 10mm and 40mm diameters. This proved top surface cooling configuration is better than the bottom with maximum heat flux. The validation showed an acceptable error margin for both surfaces with a diameter of 10mm 0.2s/^{0}C for the top surface.*

KEYWORDS: *Top and Bottom surfaces, CFD, Jet Impingement, Controlled Cooling, Lumped thermal mass, Modified ROT*

INTRODUCTION

Jet Impingement configurations have been in the research database for a long time and several kinds of configurations have been used- some bottom others inclined, and top. In all these configurations, there has been an effect on the cooling rate with regards to steel austempering in finding the best approach to minimize cost and maintain quality. The configurations produce different cooling rates, and it is imperative that the optimum configuration is known for better steel cooling. Recently, with the continual enhancement of steel material functions, the growing demand for cost-cutting by reducing the use of alloying elements, and streamlining processes: the thermo-mechanical control process (TMCP) has become increasingly important in application (Kazuaki et al., 2016) (Alqash, 2015). At one point in the designer's desired need, steel materials are subject to either of the following: bending and at the other to twisting, rotations, etc. Attending to operations under these conditions, require certain specific properties to be able to successfully withstand the various conditions the designers subject them to (Antonio et al., 2014), (Purna et al., 2013),

Print ISSN: 2055-6551(Print)
Online ISSN: 2055-656X(Online)
Website: https://www.eajournals.org/
Publication of the European Centre for Research Training and Development -UK

(Yongjun, 2015) – by restructuring its microstructure and physical structure with proper monitoring and controlling of its temperature during heating and cooling processes, hence need for a better process.

The era of Controlled cooling opens up, an important part of thermo-mechanical controlled process (TMCP) technology, which has a significant influence on the microstructure and mechanical properties of hot rolled steel plates (Qian Xie et al., 2016; Ade et al., 2011). As one of the important elements of this technology, the technique that allows the precise control of the fluid quenching temperature can be cited along with the metallurgical and controlled rolling techniques (Kazuaki et al., 2016). Therefore, jet Impingement cooling, a type of accelerated controlled cooling is a process used to achieve high heat removal yield from a heated material using a desired coolant for easy cooling**.** Steel production having desired mechanical and metallurgical properties require accurate temperature control during the cooling process (Incorpera, 2015), (Gilles et al., 2019).

A Jet impingement heat transfer cooling system was studied using water jet cooling. The impingement cooling was done for top and bottom surface stationary cooling targeting rectangular steel with single jet of different diameters. The effect of nozzle diameter and impingement gaps on convective heat transfer co-efficient h was revealed. Computational fluid dynamics (CFD) was used for simulation and validation of both models was done.

Agreeing to the Society of Automobile Engineers, and the American Institute of Steel, Iron, and steel are alloys of iron and carbon that normally have less than 1.0wt% of carbon (John, 2011). It may contain other alloying elements at different compositions and/or heat treatment (Callister et al., 2012), (Shazreena, 2013), (Khurmi et al., 2012). In this present work, we recognized three main grades of steel: low, medium, and high carbon steel with carbon content ranges of 0.015 – 0.30%wt for low carbon steel, 0.031 -0.58%wt for medium carbon steel, and 0.6 – 2%wt for high carbon steel (Incorpera, 2015).

Hydrodynamics of Jet Impingement Configuration
Jet impingement cooling process onto a solid surface with fluid occurs in different flow configurations, and different cooling systems and undergo several heat evaporation regimes as it touches the hot surface of the plate. At the run-out table (ROT) cooling stage, the fluid first exits the circular nozzle and impinges over the dry heated plate surface (free-surface jet), followed next by arrays that collide with the leftover fluid on the surface (plunging jet). In fact, these two types are mostly treated as free-surface jets in comparison with submerged jets. According to (Molana et, al, 2013). This work utilizes a free surface jet impingement cooling profile for both the top and bottom surfaces as shown in fig. 1 below.

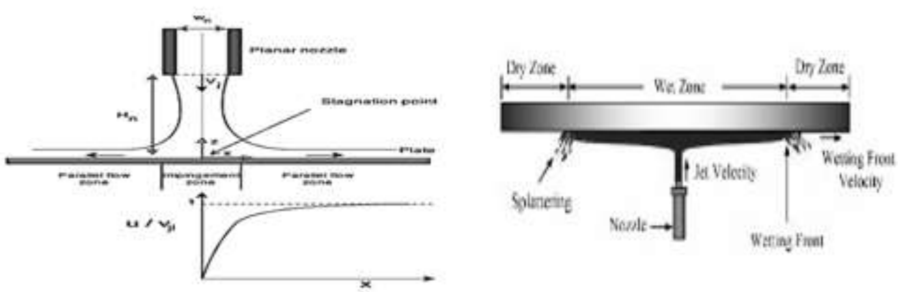

Figure 1. Schematics of free surface top and bottom jet impingement cooling models (Molana et, al, 2013)

Computational Fluid Dynamics

Numerical solution based on computational fluid dynamics (CFD) is analysis of systems involving fluid flow, heat transfer and associated phenomena such as chemical reactions by means of computer-based simulation, this technique is very powerful, spans a wide range of industrial and non-industrial application areas. (Verteeg et al., 2017), (Lokman Md et al., 2015), (Moukalled et al., 2016).

The base line results from CFD analysis are compared with experimental. Using Ansys FLUENT 2019 R3 and many other fluid flow soft wares. (Cemil et al., 2011) (Alqash, 2015), (Pallavi et al., 2017). This paper seeks to analyze two cooling process configurations- the top and bottom jet impingement cooling configuration with the aim to determining the optimum configuration, using computational fluid dynamics from a modified run-out table that handles both top and bottom surface cooling.

MATERIALS AND METHOD

An improved design run-out table was modified for the experimental runs. The run-out table housed both top and bottom surfaces as a composite on the same rig. Fig. 2 shows the improved design run-out (Onah, 2018) and modified run-out tables. Modified ROT has both top and bottom headers at the same plant while the improved design has only the top header.

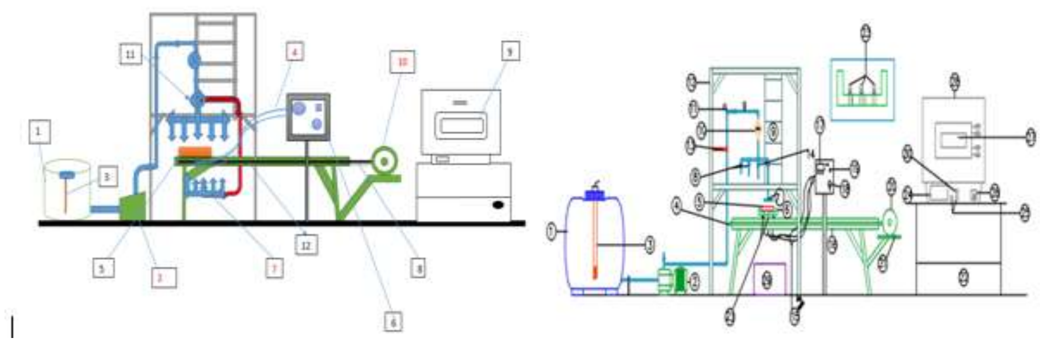

Figure 2: Schematics of Modified ROT (left) and Improved design ROT (right) set-up plant

The schematic modified ROT system set-up plant that houses the combinations of various component parts consists of 1. Water tank, 2. Electric pump, 3.Heater, 4. Thermocouple wires, 5.The workpiece and its carrier, 6.Thermocouple control panel, Workpiece bed, 7. Bottom Impingement nozzle headers, 8. Motorized screw conveyor, 9. Furnace, 10. Electric motor, 11. Flow valve/ Air attachment nozzle, 12. Flow meter, 13. Ladder, 14. Furnace support, 15, PVC Pipes, 16. Pressure gauge, 17. The location of these parts is shown on the schematic diagram in Fig.2. Pipes (PVC) - Two sets of Five PVC pipes of constant diameters of 10 and 40mm, were used shown in Fig. 3

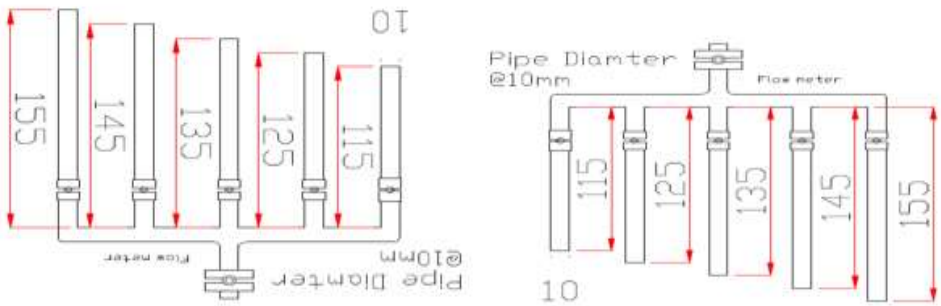

Figure 3: Diameter 10mm Bottom and Top Surface Variant H

The sample steel plates were instrumented with type-k thermocouple measuring from up to 1200ºC with an accuracy of _+ 1^0C from the bottom surface for top cooling and top surface for bottom cooling to 1mm remaining 11mm housing the thermocouple with the means of screwing and spacing of 4 thermocouples equally spaced by 50mm each along the 230mm length of the sample steel plate shown in Fig. 4

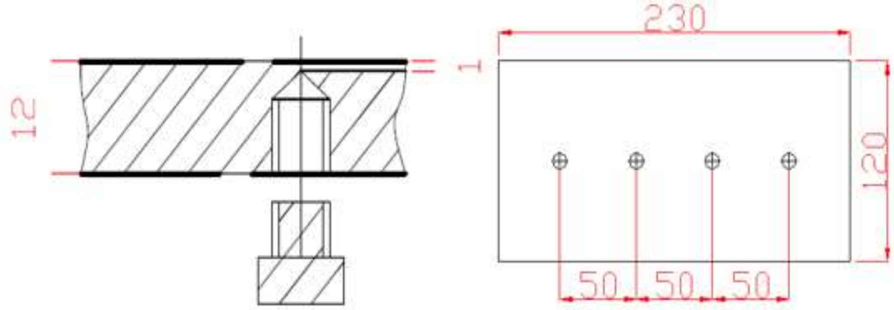

Figure 4: Steel plate instrumented with the thermocouple and its spacing

Experimental Procedure

Based on impingement diameters D=10mm and 40mm with corresponding varying impingements gaps H, of 115 and 155mm chosen from the headers of Fig. 3, two different controlled cooling temperatures of 150ºC and 110ºC were used for the experiment respectively. The following test parameters were used as experimental indictors: flow rate, nozzle velocity, constant impingement diameters, varying impingement gaps, surface temperatures range, controlled temperatures, cooling time and rate,

The sample steel plate was heated to a temperature of 750ºC to 800ºC. A tong was used to transport the hot steel plate from the furnace to Conveyor bed which took it to cooling jet. The impingement nozzle and gap headers were used to position different volume flows of water. The volume flow rate was obtained after we had opened their various meters and allowed them to stabilize. The process of flow was accurately timed at a controlled impingement cooling of 150ºC and 110ºC for 450ºC and 410ºC surface temperatures respectively. In table 1 it shows the properties of the sampled water jet impingement cooling (W-JIC) at standard temperature and pressure.

Table 1: Properties of Sampled Fluids

Fluids	Density (kg/m^3)	Viscosity (kg/M-S)	Thermal Conduct W/MK	Specific Heat J/KGK	Temp ^{0}C
W-JIC	1000	1.347x10^{-4}	0.609	500	50 - 60

Medium carbon steel plates with known varying chemical compositions and mechanical properties were obtained from Ajaokuta Nigerian Steel Company with steel grade of 0.56%C, ultimate tensile strength of 957.1Mpa and Brinnel hardness of 252.98 having impact strength of 34.11J.

Data Analysis

This model of impingement process is centered on the demonstration of transient-state heat conduction-convection across the sampled work piece thickness.

The control volume of lumped thermal mass model of the impingement process in Fig. 5 simplifies the complicated modeling process of impingement cooling which involves conduction and convection (Shankar, 2019). In this process, we assumed that: Heat transfer from the hot steel plate is seen as a lumped mass. The mass resistance to heat transfer is negligible when compared with the resistance of heat transfer with impinging fluid.

The volume of the mass remains unchanged. The 2-D heat transfer for the bottom and top surface cooling deals with a thickness of 12mm and a length of 230mm with a width of 120mm.

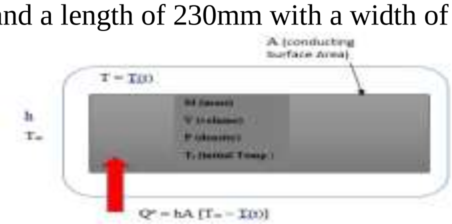

Figure 5: Control volume of lumped thermal mass model Analysis

$$MC\frac{d}{dt}(T_S - T_\infty) = -hA(T_S - T_\infty) \quad (1)$$

$$\frac{\partial(T_s - T_\infty)}{(T_s - T_\infty)} = \frac{-hAdt}{mcp} \quad (2)$$

$$\int_{t=0}^{t}\frac{d(T - T_\infty)}{T - T_\infty} = Log_e\left(\frac{T - T_\infty}{T_S - T_\infty}\right)t = 0, = \frac{-hAt}{mcp} \quad (3)$$

$$\text{Thus, } Log_\theta = \frac{-hAt}{mcp} \quad (4)$$

The gradient is given as in equation 5, as,

$$\text{gradient is } -\propto = \frac{-hAt}{mcp} \quad (5)$$

$$\text{From which, } h = \propto \rho wcp \quad (6)$$

Where h is convective heat transfer co-efficient W/m^{2}k

$for\ steel, density\ \rho = \frac{7900hg}{m^3},\ specific\ heat\ Cp = \frac{500J}{kgk};\ sampled\ thickness\ w = 0.012m, \propto,$ is gradient from equation (5)

Thereafter, a spread excel sheet used to estimate h Equation (6), where h $=\propto \rho wc$, for $\propto$ being the slope based on lumped numerical experimental temperature-time plots calculated.

Development of Numerical Simulation Model

The ANSYS fluent simulation analysis model shown was considered using the controlled temperatures of 150ºC and 110ºC for constant impingement pipe diameters of 10mm and 40mm, with corresponding constant impingement gaps of 115mm and 155mm, having element order of the mesh programmed coarse span angle center. The quality of mesh is such that the error limit is aggressive mechanical with a quality target of 0.05 having medium smoothing level, with 552 element numbers and 3321 nodes with a growth rate of 1.2. The model and output of the mesh are shown in Fig. 6.

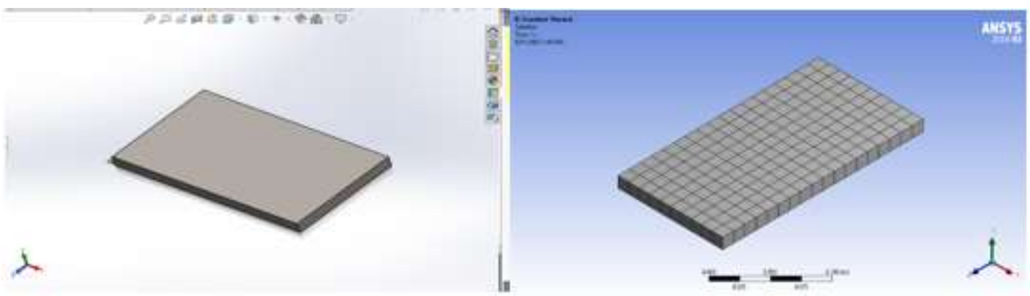

Figure 6: 3-D ANSYS Space Claim Model Geometry and Mesh model for Transient Thermal

RESULTS AND DISCUSSION

For Controlled Cooled Temperature of 110ºC, Diameter D=40mm, Results are presented in Tables 2 and 3, used for generating Fig 7 that corresponds to the top and bottom surface respectively.

Table 2: 110ºC @D=40mm Variant T and H for W-JIC Top

T=450 @D=40mm(H=115)		T=440 @D=40mm(H=125)		T=430 @D=40mm(H=135)		T=420 @D=40mm(H=145)		T=410 @D=40mm(H=155)	
T(s)	Ts	T(s)	Ts	T(s)	Ts	T(s)	Ts	T(s)	Ts
0	450	0	440	0	430	0	420	0	410
44.6	393.34	42.6	385	41	376.67	40	368.34	39.2	360
89.2	336.68	85.2	330	82	323.34	80	316.68	78.4	310
133.8	280.02	127.8	275	123	270.01	120	265.02	117.6	260
178.4	223.36	170.4	220	164	216.68	160	213.36	156.8	210
223	166.7	213	165	205	163.35	200	161.7	196	160
267.6	110	255.6	110	246	110	240	110	235.2	110

Table 3: 110ºC @D=40mm Variant T and H for W-JIC Bottom

T=450 @D=40mm(H=115)		T=440 @D=40mm(H=125)		T=430 @D=40mm(H=135)		T=420 @D=40mm(H=145)		T=410 @D=40mm(H=155)	
T(s)	Ts	T(s)	Ts	T(s)	Ts	T(s)	Ts	T(s)	Ts
0	450	0	440	0	430	0	420	0	410
66.06	393.34	64.43	385	65	376.67	60.02	368.34	59.4	360
132.12	336.68	128.86	330	130	323.34	120.04	316.68	118.8	310
198.18	280.02	193.29	275	195	279.01	180.06	265.02	178.2	260
264.24	223.36	257.72	220	260	216.68	240.08	213.36	237.6	210
330.3	166.7	322.15	165	325	163.35	300.1	161.7	297	160
396.36	110	386.58	110	390	110	360.12	110	356.4	110

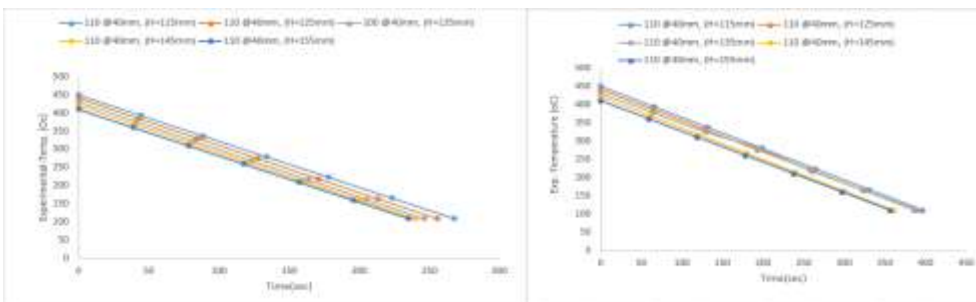

Figure 7: Top (left) and Bottom (right) Surface Temperature-Time Profile for D=40mm

From all the temperature–time plots above, irrespective of the controlled cooled temperatures, the initial surface temperatures of hot-rolled steel plate, showed the highest cooling time at gap of 115mm and lowest at the gap of 155mm, hence the choice of the two impingement gaps for further analysis.
The results revealed that it takes the top surface configuration less time to dissipate 1^0C of heat than the bottom.

Table 4: Cooling Rates of Diameters 10 and 40mm with Variant H

D(mm) and H(mm)		Cooling Rate (s/ºC) TOP	Cooling Rate (s/^{0}C) BOTTOM
	115	**1.6**	**2.56**
10	155	**1.02**	**1.93**
	115	**2.4**	**3.6**
40	155	**2.14**	**3.24**

Evaluated Convective Heat Transfer Coefficients (h) From LTMA

The results of the experiment for temperature-time were then further analyzed by lumped thermal mass analysis which showed a linear decrease from various surface temperatures to various cooling times of the form y$= -\propto x + a$ for $R^2 = b$, where $\propto$ the slope used for estimation of various convective heat transfer co-efficient h from Equation (5).

Ln (theta) For Diameter D=10mm Controlled at a temperature of 150ºC, is presented in Tables 5 and Tables 6 diameter 40mm, analyzed in Figs 8 and 9 for both top and bottom surfaces respectively

Print ISSN: 2055-6551(Print)

Online ISSN: 2055-656X(Online)

Website: https://www.eajournals.org/

Publication of the European Centre for Research Training and Development -UK

Table 5: Ln (theta) Temperature-Time Profile for D= 10mm Controlled @115°C

WATER IMPINGEMENT JET COOLING TOP					WATER IMPINGEMENT JET COOLING BOTTOM				
T=450°C @ D=10mm(H=115mm)					**T= 450 @D = 10mm(H=115mm)**				
T_s	**T_f**	**theta**	**T(s)**	**Ln(Theta)**	**T_s**	**T_f**	**theta**	**T(s)**	**Ln(Theta)**
450	50	1	0	0	450	50	1	0	0
400	50	0.875	40	-0.1335314	400	50	0.875	64	-0.13353
350	50	0.75	80	-0.2876821	350	50	0.75	128	-0.28768
300	50	0.625	120	-0.4700036	300	50	0.625	192	-0.47
250	50	0.5	160	-0.6931472	250	50	0.5	256	-0.69315
200	50	0.375	200	-0.9808293	200	50	0.375	320	-0.980839
150	50	0.25	240	-1.3862944	150	50	0.25	384	-1.38629

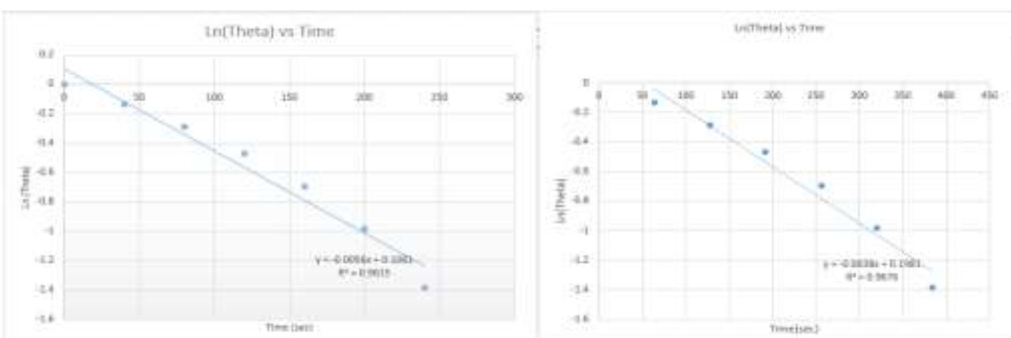

Figure 8: Ln(theta) Temperature-Time @150°C D=10mm for Top(left) and Bottom(right)

Table 6: Ln (theta) Temperature-Time Profile for D= 40mm Controlled @110°C

WATER IMPINGEMENT JET COOLING TOP					WATER IMPINGEMENT JET COOLING BOTTOM				
T= 450°C @ D = 40mm (H =115mm)					**T= 440°C @ D = 40mm (H= 115mm)**				
T_s	**T_f**	**theta**	**T(s)**	**Ln(Theta)**	**T_s**	**T_f**	**theta**	**T(s)**	**Ln(Theta)**
450	59	1	0	0	450	59	1	0	0
393.34	59	0.8550895	44.6	-0.1565491	393.34	59	0.8550895	66.06	-0.1565491
336.68	59	0.710179	89.2	-0.3422382	336.68	59	0.710179	132.12	-0.3422382
280.02	59	0.5652685	133.8	-0.5704544	280.02	59	0.5652685	198.18	-0.5704544
223.36	59	0.4203581	178.4	-0.8666484	223.36	59	0.4203581	264.24	-0.8666484
166.7	59	0.2754476	223	-1.289358	166.7	59	0.2754476	330.3	-1.289358

110	59	0.1304348	267.6	-2.0368819	110	59	0.1304348	396.36	-2.0368819

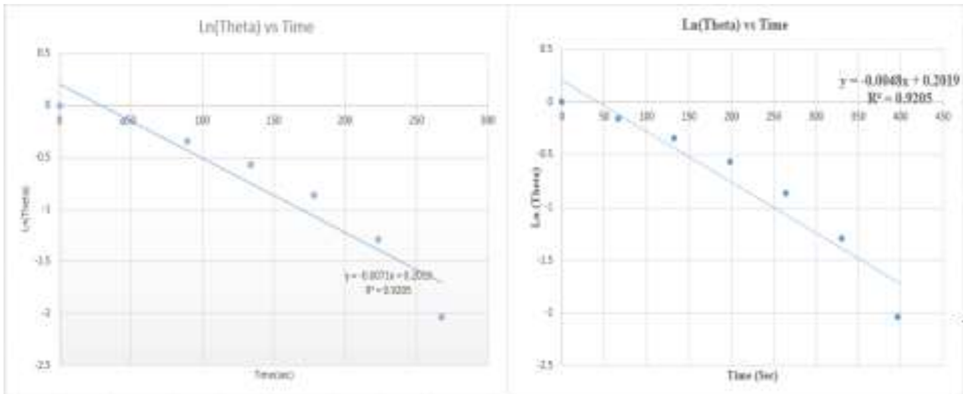

Figure 9: Ln(theta) Temperature-Time @110ºC D=40mm for Top (left) and Bottom (right)

However, in all the controlled temperatures, the values of the slope of lumped thermal mass analysis ∝, in ln(theta) temperature against time for determining convective heat transfer coefficient (h), indicated a linear increase in impingement diameter D and the corresponding increase in impingement gap H. This is suggestive that the various values of convective heat transfer coefficient (h) as obtained, would be more at higher diameter D and higher impingement gap H, for a proficient steel austempering.

Convective Heat Transfer Co-efficient h from LTMA

Table 7 showed the results of the calculated convective heat transfer coefficient (h) for D=10 and 40mm

Table 7: Calculated convective Heat Transfer co-efficient h for D=10 and 40mm

D (mm)	H (mm)	TOP h (w/m^2k)	Bottom h (w/m^2k)
	115	265.44	180.12
10	155	383.94	203.82
	115	336.54	227.52
40	155	364.98	251.22

Generally, This deduces that at any given constant pipe diameter(D), the flow rate (Q), decreases with a corresponding increase in impingement gap (H), resulting in increased convective heat transfer coefficient (h), where proficient higher heat extraction rate on hot-rolled steel plates in steel mill industry is austempered. This would achieve better microstructures of steel at controlled temperatures in the heat transfer process.

Study of Numerical Simulation Results

Figs. 11 and 12 describe the CFD temperature-time controlled cooling model of diameter 10m top and bottom surface: region 1 is a totally cooled layer of blue, region 2 middle layers are partially cooled of yellow, and region 3 red bottomed layer gradually cooled still hotter than the two layers, Also it indicates the temperature-time plot of the model, at each of the regions, the steeper curve region 1 showed where the convective heat transfer coefficient h was applied, and slowly goes down to region 2 and to region 3 where heat flow was perfectly insulated that retained some hotness in the steel plate. Figs. 13 and 14 represents the CFD-controlled heat flux model, where the top region showed the highest heat flux down to the bottom the lowest. Again, it also showed a plot of the heat flux against time for the regions.

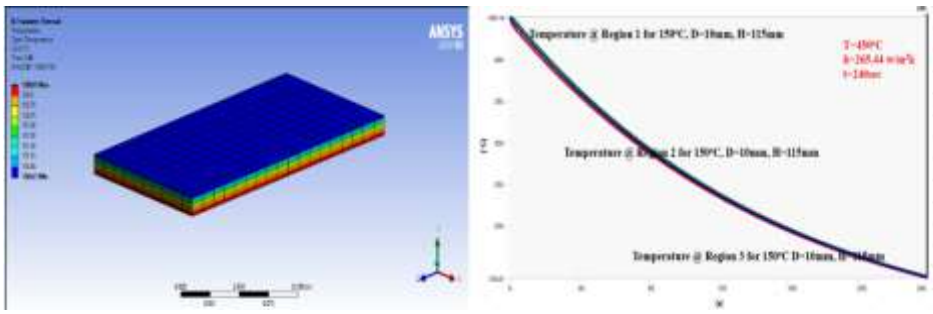

Figure 10: CFD Heat Transfer Model and Temperature-Time Profile for D=10mm Top

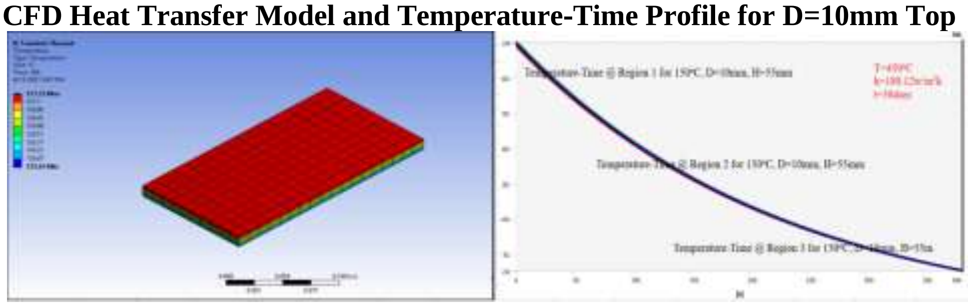

Figure 11: CFD Heat Transfer Model and Temperature-Time Profile for D=10mm Bottom

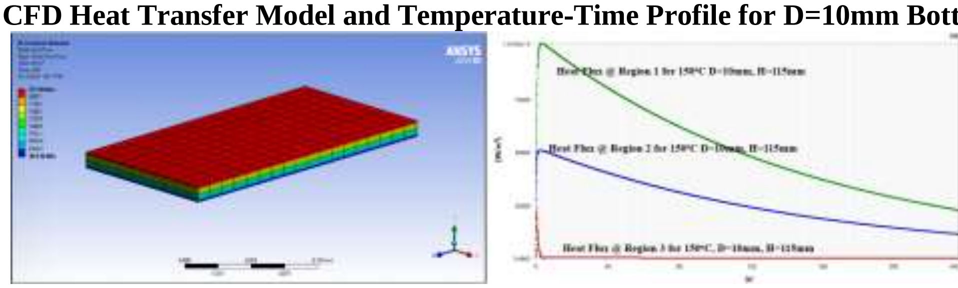

Figure 12: CFD Heat flux Model and Heat Flux –Time Plot for D=10mm Top

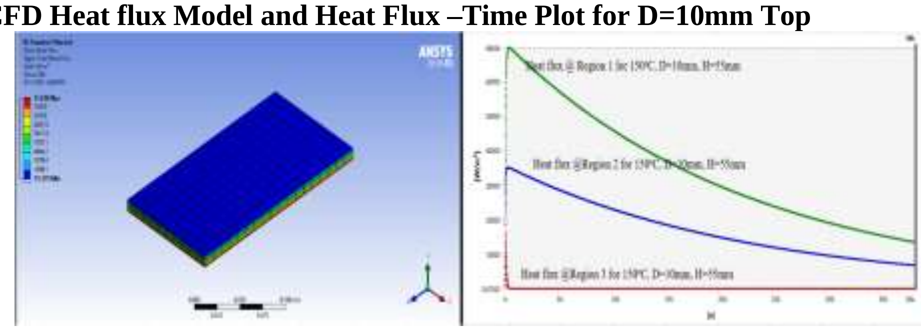

Figure 13: CFD Heat Flux Model and Heat Flux –Time Plot for D=10mm Bottom

From the Figs 10 and 11 for diameter 10mm, the highest heat flux started where convective heat transfer co-efficient h value is more. Top surface showed highest heat flux of 2518W/m^2 and bottom 13339W/m^2 which proved that top surface if 59% better impingement configuration than the bottom in 10m diameter.

Figs. 12 and 13 describe the CFD temperature-time controlled cooling model with that of diameter 40m top and bottom surface: They showed the same pattern with diameter 10mm in all the regions of the model and heat fluxes.

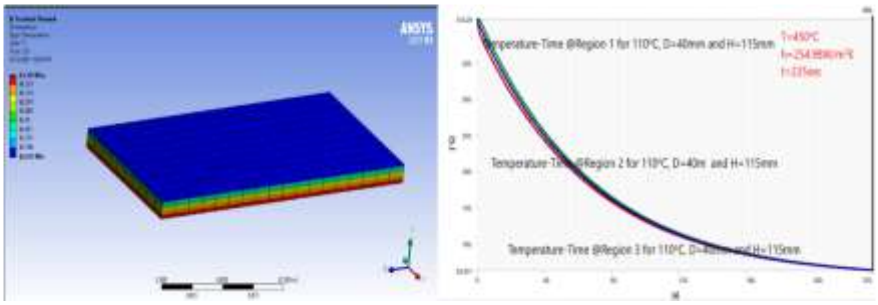

Figure 14: CFD Heat Transfer Model and Temperature-Time Profile for D=40mm Top

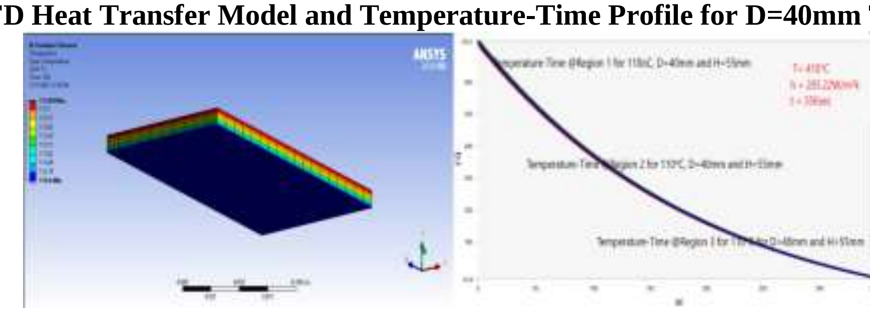

Figure 15: CFD Heat Transfer Model and Temperature-Time Profile for D=40mm Bottom

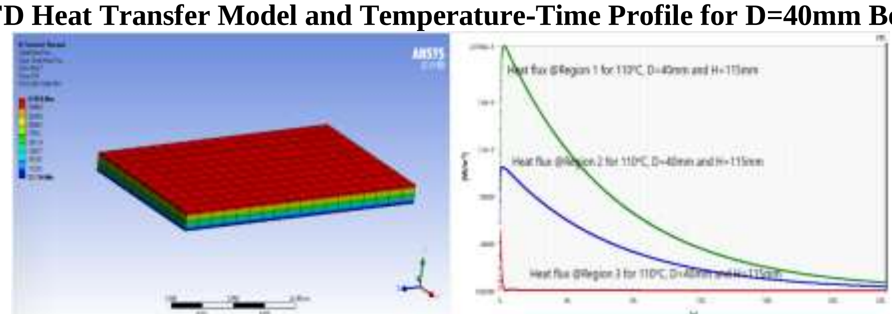

Figure 16: CFD Heat flux Model and Heat Flux –Time Plot for D=40mm Top

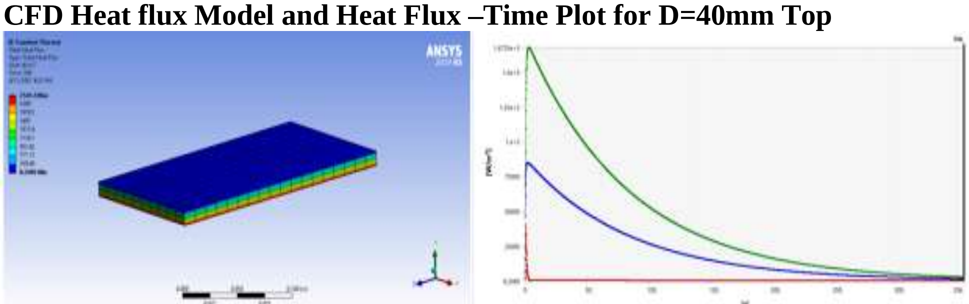

Figure 17: CFD Heat Flux Model and Heat Flux –Time Plot for D=40mm Bottom

From the Figs 16 and 17 for diameter 40mm, the highest heat flux started where convective heat transfer co-efficient h value is more. Top surface showed maximum heat fluxes of 6742.8W/m^2 and bottom 2541.4W/m^2 which again proved that top surface if 38% better impingement configuration than bottom in diameter 40mm.

Validation of the experimental and simulated data shown in table 10 used in generating fig. 18

Table 8: Top and Bottom Surface Experimental Data

Top 10		Bottom 10		Top 40		Bottom 40		Top 10		Bottom 10		Top 40		Bottom 40	
t(s)	Ts ^{o}C	t(s)	Ts ^{o}C	t(s)	Ts ^{o}C	t(s)	Ts ^{o}C	t(s)	Ts ^{o}C	t(s)	Ts ^{o}C	t(s)	Ts ^{o}C	t(s)	Ts ^{o}C
EXPERIMENTAL DATA								**SIMULATION DATA**							
0	450	0	450	0	410	0	410	1.00E-02	449.78	1.00E-02	450.02	1.00E-02	410	1.00E-02	410.06
40	400	64	400	39.2	360	59.4	360	40	355.02	64	355	39.02	342	59.44	328
80	350	128	350	78.4	310	118.8	310	80	286.78	128	291.33	78.44	296	118.84	296.44
120	300	192	300	117.6	260	178.2	260	120	233.91	192	225.57	117.64	230.6	178.01	225.7
160	250	256	250	156.8	210	237.6	210	160	192.95	256	183.36	156.84	189.8	237.64	191.43
200	200	320	200	196	160	297	160	200	161.21	320	151.42	196	134.8	297	128
240	150	384	150	235.2	110	356.4	110	240	136.61	384	127.25	235	89	356	85

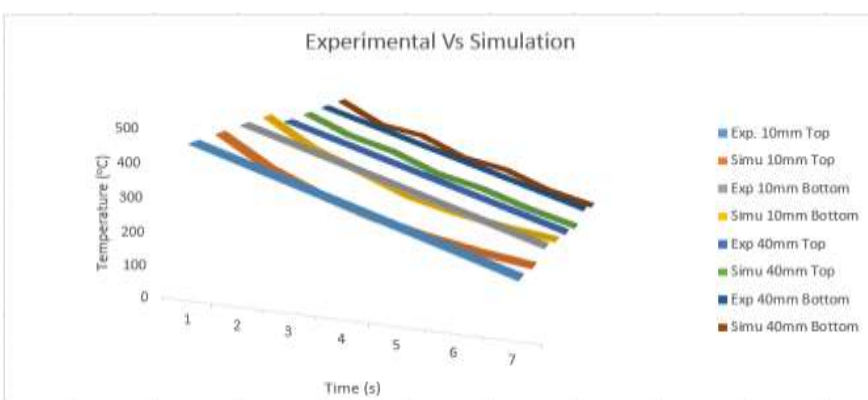

Figure 18: Comparative study of Temperature-Time Plot for Top and Bottom

From the validation of the temperature-time plot of both analysis, it showed an acceptable error of margin of 0.2s/^{0}C and 0.4s/^{0}C cooling rate for diameter 10mm of top and bottom surface respectively. While Diameter 40mm also an acceptable error margin of 0.5s/^{0}C and 1s/^{0}C cooling rate for the top and bottom surfaces respectively. Evident again in the validation top surface still showed less error.

CONCLUSIONS

This study involves the comparative analysis of top and bottom surface jet impingement-controlled cooling configurations. Empirical results revealed from the temperature-time plot that, for diameter 10mm top surface showed better controlled cooling by 63% and 53% difference. Also in diameter 40mm top surface maintained better controlled cooling with67% and 66% at the two variant impingement gaps respectively. From the calculated convective heat transfer coefficient h, it also revealed 265.44w/m^{2}k and 180.12w/m^{2}k for 115mm and 383.94w/m^{2}k and 203.82w/m^{2}k for 155mm impingement gaps of diameter 10mm for top and bottom respectively. Also, 336.54w/m^{2}k and 227.52w/m^{2}k for 115mm and 364.98w/m^{2}k and 251.22w/m^{2}k for 155mm impingement gaps of diameter 40mm for top and bottom surface controlled cooling respectively. Generally, it suggests that convective heat transfer coefficient (h) increases with increase in pipe diameter (D) with corresponding increase in impingement gaps (H) in both cooling processes. This deduces that at any given impingement heat transfer process top surface cooling configuration has higher proficient heat extraction rate on hot-rolled steel which would achieve better microstructures of steel at controlled temperature in heat transfer process.

CFD numerical simulation maximum heat fluxes were 22518W/m^2 and 6742.8w/m^2 at top surface, while bottom maintained minimum with 13339w/m^2 and 2541.4w/m^2 for both 10mm and 40mm diameters respectively. The top surface showed better heat flux than the bottom

The validation showed an acceptable error margin for both surfaces with diameters 10mm 0.2s/^{0}C and 0.4s/^{0}C and 0.5s/^{0}C and 1s/^{0}C at diameters 40mm for the top and bottom respectively. The top surface also showed less error than the bottom. The top surface cooling configuration stands for a better cooling configuration than the bottom as it extracts higher heat from the hot surface.

Conflicts of Interest
There are no conflicts of interest in this work

Funding
This work was not funded by any organization.

REFERENCES

Ade et al., A. (2011). Effect of Heat Treatment on the Mechanical Engineering Essay. *1st International Conference on Experiments/process/system Modelling/Simulation/Optimization Intelligence. 11*, pp. 517 -529. London: Essays Engineering. Retrieved from www.ukessays.com

Alqash, S. I. (2015). Numerical Simulations of Hydrodynamics of multiple water jet impinging over a horizontal moving plate. In *Numerical Simulations of Hydrodynamics of multiple water jet impinging over a horizontal moving plate* (p. 125). Vancouver: University of British Columbia, Vancouver.

Antonio et al. (2014). Accelerated Cooling of Steel Plates: The Time has Come. *Journal of ASTM International, 5*, 8 - 15.

Callister et al. (2012). *Phase Transformation of Microstrutural Formation from Austenite.*

Cemil et al. (2011). Experimental Measurement and Computational Modeling for the Spray Cooling of a Steel Plate Near the Leidenfrost Temperature. *Journalof Thermal Science and Technology*(31), 27 -36.

Gilles et al. (2019). Modeling of Transient Bottom Jet Impingement Boiling. *Elesevier International Journal of Heat and Mass Transfer*, 1160-1170.

Incorpera. (2015). *Advances in Heat Transfer.* Academic press.

Jeffery, A. (2011). *Advanced Engineering Mathematics.* Academic Press.

John, M. (2011). *http://www.efunda.com/materials/alloys/carbon steel/carbon film*.

Kazuaki et al. (2016). Water Quenching CFD (Computational Fluid Dynamics) Simulation with Cylinderical Impinging Jets. *NIPPON Stell and SUMITOMO Metal Technical Report, no III*, pp. 621 - 771. Osaka.

Khurmi et al. (2012). *Theory of Metal on Carbon Steels and Mechanical Properties of Medium Carbon Steel.*

Lokman Md et al. (2015). Literature Review of Accelerated CFD Simulation Methods towards Online Application. *The 7th International Conference on Applied Energy , Elsevier Energy Procedia*(75), 3307-3314.

Molana et al. (2013). Investigation of Heat Transfer Processes Involved Liquid Impingement Jets: A Review. *Brazilian Journal of Chemical Engineering, 30*(03), 413-435.

Molana et, al. (2013). Investigation of Heat Processes Onvolved in Liquid Impingement Jets: A Review. *Brazilian Journal of Chemical Engineering, 03*(30), 413 - 435.

Moukalled et al. (2016). *Finite Volume Method in Computational Fluid Dynamics, Advanced Introduction with OpenFOAM and Matlab.* Switzerland: Springer International.

Onah. (2018). *Improved Design and Parametric Study of Controlled Water Jet Impingement Colling System for Hot Rolled Steel Plates Using Mechanistic Modeling.* Enugu: Postgraduate studied of Enugu state university of Science and Technology.

Pallavi et al. (2017). Experimental and CFD Analysis of Jet Impingement Cooling on Copper Circular Plate. *World Journal of Engineering and Research and Technology, III*(5), 256-267.

Purna et al., P. (2013). Model Based Numerical State Feedback Control of Jet Impingement Cooling of a Steel Plate by Pole Placement Technique. *International Journal of Computational Engineering Research, 03*(8), 2205-3005.

Qian Xie et al. (2016). Heat Transfer Coefficient and Flow Charateristic of hot Steel Plates Cooling by Multiple Inclined Impinged Jets. *ISIJ International*.

Shankar, R. S. (2019). Unsteady Heat Transfer: Lumped Thermal Capacity Model. clarkson university.

Shazreena, B. S. (2013). *Effect of Heat Treatment on the Microstructure and Mechanical Properties of low carbon Steel* (Vol. II).

Verteeg et al. (2017). *An Introduction to Computational Fluid Dynamics: The Finite Element Method.* Edinburgh: Pearson Education Publishing.

Yongjun, Z. (2015). *The Cooling of a Hot Steel Plate by Impinging Water Jet.* Wollongong university.